THE JOURNAL OF BIOLOGICAL CHEMISTRY
Vol. 273, No. 40, Issue of October 2, pp. 25616–25627, 1998

Printed in U.S.A.

Identification of Sorting Determinants in the C-terminal Cytoplasmic Tails of the γ-Aminobutyric Acid Transporters GAT-2 and GAT-3*

(Received for publication, March 25, 1998, and in revised form, July 17, 1998)

Theodore R. Muth‡§, Jinhi Ahn, and Michael J. Caplan

From the Departments of Cellular and Molecular Physiology and ‡Cell Biology, Yale University School of Medicine, New Haven, Connecticut 06520

In order to perform their physiologic functions, polarized epithelial cells must target ion transport proteins to the appropriate domains of their plasma membranes. Molecular signals responsible for polarized sorting have been identified for several membrane proteins which span the bilayer once. Most ion transport proteins are polytopic, however, and little is known of the signals responsible for the targeting of this class of polypeptides. Members of the γ-aminobutyric acid (GABA) transporter family are polytopic membrane proteins found endogenously in both epithelial cells and neurons. We have identified narrowly defined sequences which are required for the proper accumulation of two members of this transporter family in Madin-Darby canine kidney cells. The highly homologous GABA transporter isoforms, GAT-2 and GAT-3, localize to the basolateral and apical surfaces, respectively, when expressed stably in Madin-Darby canine kidney cells. We have generated deletion constructs and chimeric transporters composed of complimentary portions of GAT-2 and GAT-3. We find that information which directs their differential sorting is present in the C-terminal cytoplasmic tails of these two polypeptides. A sequence of 22 amino acids at the C terminus of GAT-2 is required for the transporter's basolateral distribution and is capable of directing GAT-3 to the basolateral surface when appended to the C terminus of this normally apical polypeptide. The deletion of 32 amino acids from the C terminus of GAT-3 causes this transporter to become mislocalized to both surfaces. Moreover, removal of the final three amino acids of GAT-3 (THF) similarly disrupts its apical sorting. The GAT-3 C-terminal sequence resembles motifs which interact with PDZ domains, raising the possibility that the steady state distribution of GAT-3 at the apical plasmalemmal surface requires a protein-protein interaction mediated by its extreme C-terminal cytoplasmic tail. These data provide the first characterization of a protein-based signal required for the apical distribution of a membrane protein.

To generate their functionally distinct plasma membrane domains, polarized cells must be able to confine specific proteins to their appropriate locations (1). Epithelia and neurons are well studied examples of polarized cells whose structural designs are especially geared toward maintaining compositionally discrete membrane surfaces (2, 3). In order to achieve their proper distributions in these cell types, membrane proteins must be endowed with sorting signals which specify their sites of functional residence (4–11). Presumably, sorting signals are recognized by components of a cell's sorting machinery which act upon the targeting instructions they encode.

The task of sorting proteins to specific membrane surface domains is accomplished by all polarized cells (1, 3). It is unclear, however, if all polarized cell types utilize a universal sorting machinery or if divergent mechanisms operate in different cell types. Studies of viral glycoprotein targeting have led to the suggestion that neurons and epithelia may employ similar signals and mechanisms to generate polarized protein distributions (2, 12, 13). Furthermore, these studies suggested that proteins sorted to the apical surfaces of epithelia accumulate in the axons of neurons, while proteins of the epithelial basolateral membrane are restricted to the somatodendritic regions of the neuronal plasmalemma (2). While there are clearly exceptions to this model (14–16), it has provided a useful paradigm which has guided investigations into those elements of the sorting process that are shared among diverse polarized cell types.

The relationship between membrane protein sorting in epithelia and neurons has been further examined through studies employing members of the GABA[1] neurotransmitter transporter family (17, 18). There are four closely related GABA transporters, GAT-1, GAT-2, GAT-3, and the betaine transporter, BGT-1 (17, 19, 20). The GABA transporters expressed in neurons are responsible for removing the inhibitory neurotransmitter GABA from the synaptic cleft after it has been released from the presynaptic terminal (21, 22). Consistent with this function, the GAT-1 isoform has been localized to the axons of hippocampal neurons *in situ* and in culture (23, 24). From this position, GAT-1 can limit the diffusion of GABA and serve to terminate its inhibitory signaling by reimporting the transmitter into the axon terminus, where it can be recycled into synaptic vesicles (21, 22, 25).

When expressed by transfection in the polarized canine kidney epithelial cell line, MDCK, GAT-1 and GAT-3 are sorted to the apical surface whereas GAT-2 and the BGT-1 transporter are restricted to the basolateral domain (23, 26). In transfected cultured hippocampal neurons, BGT-1 is restricted to somatodendritic surfaces, while GAT-3 can gain access to the axons

* This work was supported by National Institutes of Health Grant GM42136, a National Science Foundation National Young Investigator Award (to M. J. C.), and a National Institutes of Health pre-doctoral fellowship (to T. R. M.). The costs of publication of this article were defrayed in part by the payment of page charges. This article must therefore be hereby marked "*advertisement*" in accordance with 18 U.S.C. Section 1734 solely to indicate this fact.

§ To whom correspondence should be addressed. Tel.: 203-785-6833; Fax: 203-785-4951; E-mail: Tmuth@biomed.med.yale.edu.

[1] The abbreviations used are: GABA, γ-aminobutyric acid; GAT, GABA transporter; MAGUK, membrane-associated guanylate kinase; BGT, betaine transporter; PBS, phosphate-buffered saline; MDCK, Madin-Darby canine kidney; FITC, fluorescein isothiocyanate.

(26). It would appear, therefore, that these transporters encode sorting information which is interpretable by both neuronal and epithelial protein sorting machinery.

In this study we have generated deletion constructs and chimeras of the GAT-2 and GAT-3 transporters in order to determine which protein sequence domains specify membrane targeting in MDCK cells. We find that both GAT-2 and GAT-3 manifest sorting information in their C-terminal cytoplasmic tails. A GAT-2 transporter lacking its C-terminal 22 amino acids is no longer strictly basolateral, but instead is predominantly apical. Additionally, when these 22 amino acids are substituted in place of the GAT-3 C-terminal amino acids, this chimeric transporter accumulates entirely basolaterally, suggesting that these C-terminal residues of GAT-2 contain dominant basolateral sorting information. Likewise, when the C-terminal 32 amino acids of GAT-3 are removed, the resultant truncated transporter is no longer polarized to the apical surface, but is instead found at both surfaces in roughly equal amounts. It would appear, therefore, that both of these GABA transporters embody sorting signals in their cytoplasmic C-terminal tails. Examination of the sequences of these tails suggests that distinct classes of cellular sorting machinery may recognize these signals and act upon their encoded targeting instructions.

EXPERIMENTAL PROCEDURES

Plasmid Constructions—The clones for GAT-2 and GAT-3 were a kind gift of L. Borden. All GAT cDNAs were subcloned into the mammalian expression vector, pCB6, at the *Cla*I and *Xba*I restriction sites. GAT-3 c-Myc was generated by polymerase chain reaction using primers coding for the EQKLISEEDL c-Myc epitope tag as described (26). GAT-3 Δ32 was generated by inserting an oligonucleotide linker into the GAT-3 sequence between the *Hin*dIII site in GAT-3 and the *Xba*I site in the pCB6 polylinker. This manipulation was complicated by the presence of *Xba*I sites both 5′ and 3′ of the GAT-3 insert in the pCB6 vector. This caused a GAT-3 fragment with a 5′ *Xba*I overhang and a 3′ *Hin*dIII site to be released from the pCB6 vector. This fragment was isolated and the linker described below was ligated to the *Hin*dIII site (the linker was designed such that its *Xba*I overhang was only exposed after it was cut with *Xba*I). The modified fragment was then cut with *Xba*I so that it now had *Xba*I overhangs at both the 5′ and 3′ ends. This fragment was then cloned into the pCB6 vector at the *Xba*I and clones screened for insertions with the correct orientation. The linker was formed by annealing the following oligos, 5′-CTAGAGAATTCCTAA-3′ and 5′-AGCTTTAGGAATTCT-3′. The linker introduces a stop codon after residue 595, truncating the last 32 amino acids. GAT-3 Δ40N was generated by inserting a linker between the *Xba*I site 5′ of GAT-3 and the *Drd*I site just prior to residue 40 of GAT-3. Again, because of the presence of *Xba*I sites at both 5′ and 3′ ends of the GAT-3 insert, cutting with *Xba*I and *Drd*I released a GAT-3 fragment with *Drd*I and *Xba*I overhangs from pCB6. As above, the linker was ligated to the *Drd*I overhang at the 5′ end of this fragment, the modified fragment cut with *Xba*I to expose the 5′ *Xba*I overhang and then cloned back into pCB6 at the *Xba*I site. Clones were screened for insertions with the correct orientation. The oligonucleotide linker was formed by annealing the oligos 5′-CGCGCCGGCGAATTCTAGACCATGG-3′ and 5′-ATGGTCTAGAATTCGCCGGCGCG-3′. This linker encodes an in-frame Kozak consensus start site, a methionine, and follows with the alanine residue at position 41 of GAT-3. GAT-3/C2 was generated by inserting a linker between the *Hin*dIII site of GAT-3 and the *Xba*I site of the pCB6 polylinker. The oligos used to generate this linker were 5′-AGCTCGAGCTGACTTCTCCAGCGACACCGATGACGTCCCTCCTCAGGCTCACAGAACTGGAGTCTAACTGCTAGT-3′ and 5′-CTAGACTAGCAGTTAGACTCCAGTTCTGTGAGCCTGAGGGACGTCATCGGTGTCGCTGGAGAAGTCAGCTCG-3′. The linker codes for the last 22 amino acids and stop codon of GAT-2. GAT-2/C3 was generated by inserting an oligo linker between the *Apa*I site of GAT-2 and the *Xba*I site of the pCB6 polylinker. Annealing oligos 5′-CACTCAGAGAGAGACTTCGCCAGCTCGTGTGCCCGGCTGAAGACCTTCCCCAGAAGAGCAAGCTTTGAGGGGCGGCCGCCCGAATTCT-3′ and 5′-CTAGAGAATTCGGGCGGCCGCCCCTCAAAGCTTGCTCTTCTGGGGAAGGTCTTCAGCCGGGCACACGAGCTGGCGAAGTCTCTCTCTGAGTGGGCC-3′ formed the linker. This linker codes for GAT-2 sequence up to amino acid position 578 of GAT-2 and then codes residues 594 and 595 (Lys and Leu) of GAT-3. Insertion of the linker added a *Hin*dIII site in the intermediate construct. The GAT-2/C3 intermediate was then cut with *Hin*dIII and *Eco*RI and the *Hin*dIII/*Eco*RI fragment of GAT-3, coding for the last 34 amino acid residues and stop codon of GAT-3, was inserted. The final construct encodes the GAT-2 transporter with its last 24 amino acids replaced by the last 34 amino acids of GAT-3. GAT-2 Δ24 was prepared similarly to GAT-2/C3 using an oligonucleotide linker formed by annealing the following oligos, 5′-CACTCAGAGAGAGACTTCGCCAGCTCGTGTGCCCGGCTGAAGACCTTCCCCAGAAGAGCTGAGGGGCGGCCGCCCGAATTCT-3′ and 5′-CTAGAGAATTCGGGCGGCCGCCCCTCAGCTCTTCTGGGGAAGGTCTTCAGCCGGGCACACGAGCTGGCGAAGTCTCTCTCTGAGTGGGCC-3′. This linker codes for a stop codon which truncates the GAT-2 transporter following residue 578. GAT-3 THF$^-$ was generated by inserting a linker into GAT-3 between the *Kpn*I site in the 3′ end of GAT-3 and the *Xba*I site in the pCB6 polylinker. The following oligos were used to generate the linker, 5′-CATCTCTGCCACACAGAGAAGGAGTGAAT-3′ and 5′-CGATTCACTCCTTCTCTGTGATGGCAGAGATGGTAC-3′. The oligo linker codes for GAT-3 sequence up to residue 624 and then adds a stop codon that truncates the last three amino acid residues.

All restriction digests were performed using New England Biolabs (Beverly, MA) restriction enzymes according to the manufacturer's protocol. All DNA fragments were isolated using the GeneClean II (Bio 101 Inc., Vista, CA) system. All DNA constructs were grown in DH5α *Escherichia coli* and DNA was isolated using Promega (Madison, WI) Miniprep or Maxiprep systems. Life Technologies, Inc. (Grand Island, NY) competent DH5α *E. coli* were used for all transformations. All GAT-3 and GAT-2 constructs were sequenced through the relevant junction sites to confirm their integrity. All oligos were prepared by the Keck facility at Yale University and were annealed by heating to 95 °C in annealing buffer (250 mM Tris-HCl, 100 mM $MgCl_2$, pH 8.0), and cooling slowly to 25 °C.

Cell Culture and Transfection—MDCK cells were grown in minimal essential medium (Life Technologies, Inc.) with 10% fetal calf serum (Sigma) and 50 units/ml penicillin and 50 units/ml streptomycin (Life Technologies, Inc.) at 37 °C and 5% CO_2. Transfections were performed using Ca_2PO_4 precipitation with 60 mg of cDNA followed by selection in Geneticin (0.9 g/liter) (Life Technologies, Inc.). Resistant colonies were isolated using cloning rings (Bellco Glass Inc., Vineland, NJ) following 7 to 10 days of selection. Clones were initially screened for expression using a modified GABA transport assay (see below) and the positive cell lines were confirmed using indirect immunofluorescence with the appropriate GABA transporter antibodies.

Immunofluorescence Microscopy—The primary antibody R22, used to detect GAT-2, was kindly provided by R. Jahn and L. Edelmann (Yale University). The GAT-3-specific antibodies 669 (N-terminal) and 670 (C-terminal) were kindly provided by B. Kanner (The Hebrew University). The anti-Na,K-ATPase α subunit antibody, 6H, has been described previously (14). The anti-c-Myc antibody, 9E10, was a kind gift of S. Goldstein (Yale University).

Immunofluorescence experiments were performed as described previously (26). Briefly, MDCK cells were grown on Costar 24-mm Transwell filter supports (Corning Costar, Cambridge, MA) for 7 days prior to the day of the experiment. Filters were excised from the filter rings and the cell monolayers were washed twice in PBS with calcium (0.1 mM $CaCl_2$) and magnesium (1.0 mM $MgCl_2$) (PBS-Ca/Mg) and then fixed in −20 °C methanol for 9 min. Cell monolayers were rinsed in PBS-Ca/Mg and then incubated in permeabilization buffer (PBS-Ca/Mg, 0.3% Triton X-100, and 0.1% bovine serum albumin) for 15 min. Monolayers were then blocked for 30 min in goat serum dilution buffer (16% filtered goat serum, 0.3% Triton X-100, 20 mM NaP_i, pH 7.4, 150 mM NaCl) to reduce nonspecific IgG-binding sites (27). Cell monolayers were then incubated with primary antibodies diluted in goat serum dilution buffer in a humidifying box for 1 h at room temperature or overnight at 4 °C. The cells were rinsed 3 times for 5 min in permeabilization buffer and then incubated with secondary antibodies, FITC-conjugated anti-rabbit IgG, or rhodamine-conjugated anti-mouse IgG (Sigma), diluted in goat serum dilution buffer for 1 h at room temperature in a humidifying box. The cells were washed as described above in permeabilization buffer and for an additional 10 min in 10 mM NaP_i, pH 7.5. The cells on filters were mounted on a glass slide using Vectashield (Vector Laboratories, Burlingame, CA) or freshly prepared mounting solution (75% glycerol/PBS with 0.1% *p*-phenylenediamene). A coverslip was placed over the filter sections and sealed with nail polish.

Immunofluorescent images were generated using a Zeiss (Oberkochen, Germany) LSM 410 laser scanning confocal microscope. Contrast and brightness settings were chosen to ensure that all pixels were within the linear range. Images are the product of 8-fold line

FIG. 1. **Sequences of GABA transporter construct C termini.** This figure shows the C-terminal amino acid sequences of GAT-2, GAT-3, and of the various GAT-2 and GAT-3 deletion and chimeric constructs generated for these studies. GAT-3, GAT-3 c-Myc, GAT-3/C2 and GAT-3 THF$^-$ sequence begins 10 amino acids after the predicted 12th transmembrane domain, whereas the GAT-2, GAT-2 Δ24, and GAT-2/C3 sequences commence at the predicted boundary of the transmembrane domain. The *numbers* indicate position in the amino acid sequence. *Black lettering* represents GAT-2 sequence while *gray text* represents GAT-3 sequence. *Underlined text* denotes the c-Myc epitope tag. GAT-3 Δ40N is not shown.

averaging. The *xz* cross-sections were produced using a 0.2-μm motor step.

[^{3}H]GABA Transport Assay—Transport assays were performed as described previously (26), with a few modifications. Briefly, MDCK cells stably expressing a GABA transporter construct were grown on 6.5-mm Costar Transwell filter supports. Cells were plated at an initial density of 4.0×10^4 per filter and allowed to grow under standard conditions for 1 week. Cells were rinsed 3 times with PBS-Ca/Mg and then incubated with a solution containing [^{3}H]GABA at a final concentration of 50 nM (0.33 mCi/ml) for 12 min at room temperature. One hundred-fold excess unlabeled GABA was present at the surface not being assayed for GABA transport activity. The filters were rinsed 3 times in ice-cold PBS-Ca/Mg, excised from the supports, and placed in scintillation vials with 800 μl of lysis buffer (1% SDS) for 10 min with gentle horizontal shaking. A 200-μl aliquot of this lysate was removed for use in a protein assay and the remaining 600 μl was mixed well with 5 ml of EcoLume (ICN, Costa Mesa, CA) and counted in a scintillation counter. Each cell line was assayed in triplicate or quadruplicate with background transport measured in duplicate samples. Combined apical and basolateral background counts were subtracted from the total GAT transporter associated counts prior to calculating the transporter activity. Transport activity was measured in picomole of GABA transported per μm^2 of cell monolayer assayed. All chemicals used are from J. T. Baker (Philipsburg, NJ) unless otherwise noted.

RESULTS

Importance of the C-terminal Cytoplasmic Tail for the Apical Localization of GAT-3—Our initial studies of the distribution of GAT-3 in MDCK cells made use of specific antibodies directed against this transporter kindly provided by B. Kanner (26). For subsequent experiments we chose to epitope tag the transporter with the short 10 amino acid c-Myc sequence (EQKLISEEDL). A tagged GAT-3 construct was designed to carry the epitope tag at the extreme C terminus, leaving all 627 amino acids of GAT-3 intact (Fig. 1). GAT-3 c-Myc transiently expressed in COS-1 cells reaches the cell surface and is capable of mediating GABA transport (data not shown). Stably transfected MDCK cells expressing GAT-3 c-Myc transporters also deliver them to the plasma membrane, where they are able to transport GABA. To assess the surface distribution of the tagged transporters, several independently generated GAT-3 c-Myc expressing MDCK lines were grown to confluence on Costar Transwell filters and then examined by indirect immunofluorescence confocal microscopy using the N-terminal-specific GAT-3 antibody 669. Surprisingly, all clones of GAT-3 c-Myc examined (more than 10 independent clones) distribute GAT-3 c-Myc roughly equally between both apical and basolateral membrane surfaces (Fig. 2, *e* and *f*). This is distinctly different from wild type GAT-3, which is almost entirely apical (Fig. 2, *a* and *b*)(26). The basolateral marker, Na,K-ATPase α subunit, remains basolateral in MDCK cells stably expressing GAT-3 (Fig. 2, *c* and *d*) as well as all of the other GAT constructs examined in these studies (data not shown). The apical and basolateral distribution of GAT-3 c-Myc is observed both

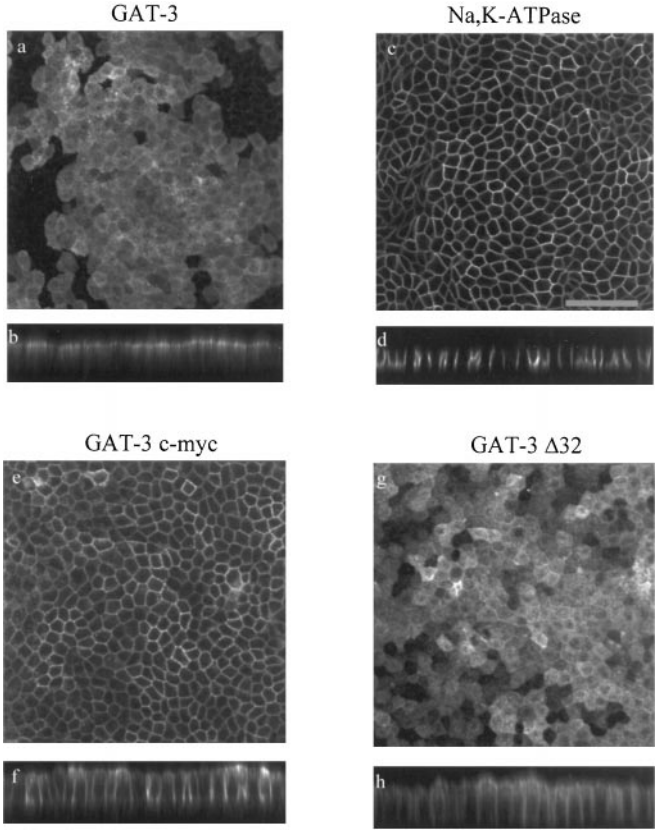

FIG. 2. **Cell surface distribution of GAT-3 c-Myc and GAT-3 Δ32 determined by immunofluorescence.** MDCK cells were stably transfected with GAT-3, GAT-3 c-Myc, or GAT-3 Δ32 in the pCB6 mammalian expression vector. *a* and *b* show confocal en face and *xz* cross-section images, respectively, of cells that were stained for the GAT-3 transporter using the GAT-3 specific antibody 669. GAT-3 is predominantly at the apical surface of polarized MDCK cells. *c* and *d* show en face and *xz* section images of the same field of GAT-3 expressing cells shown in *a* and *b* costained for the α subunit of the Na,K-ATPase using the 6H monoclonal antibody. In this cell line, and all others examined, the Na,K-ATPase α subunit is polarized to the basolateral surface. *e* and *f* show en face and *xz* section images of cells that were stained for the GAT-3 c-Myc transporter using the GAT-3 specific antibody 669. *g* and *h* show en face and *xz* section images of cells that were stained for the GAT-3 Δ32 transporter using the GAT-3 specific antibody 669. Unlike the wild type GAT-3, both GAT-3 c-Myc and GAT-3 Δ32 are present at the apical and basolateral surfaces of MDCK cells in roughly equivalent amounts. All cells stained for GAT-3 were labeled fluorescently with FITC-conjugated anti-rabbit secondary antibodies while the Na,K-ATPase α subunit was fluorescently labeled using rhodamine-conjugated anti-mouse secondary antibodies. *Bar* equals 50 μm.

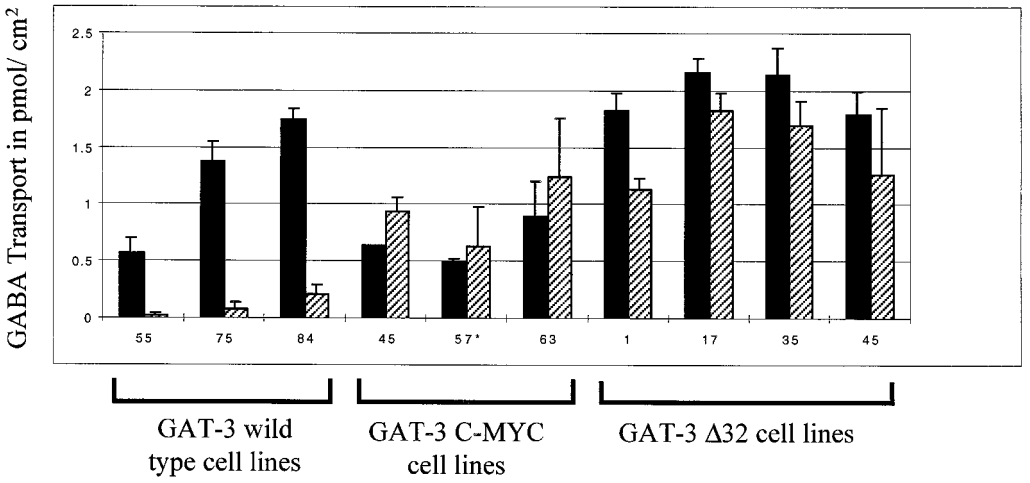

FIG. 3. **GABA transport by cells expressing GAT-3, GAT-3 c-Myc, or GAT-3 Δ32.** Confluent monolayers of MDCK cell lines stably expressing GAT-3, GAT-3 c-Myc, or GAT-3 Δ32 were grown on 6.5-mm Costar Transwell filter supports for 1 week and then incubated with 50 nM [^{3}H]GABA (0.33 mCi/ml) from either the apical (■) or basolateral (▨) surface for 12 min at room temperature. GABA uptake was determined by measuring cell-associated counts. Nonspecific transport was determined by incubating GAT transporter expressing cells in 0.5 mM unlabeled GABA under otherwise standard transport conditions. The first set shows GABA transport activity of wild type GAT-3 cell lines, which is detected predominantly at the apical surface. The apical to basolateral transport ratios are consistent with previously published results. The second and third sets of results show GABA transport activity of GAT-3 c-Myc and GAT-3 Δ32 cell lines, respectively. In contrast to the wild type GAT-3 expressing cell lines, GAT-3 c-Myc and GAT-3 Δ32 cell lines have roughly equivalent levels of GABA transport activity at both the apical and basolateral surfaces. *Asterisk* indicates the average of two independent experiments.

when GAT-3-specific antibodies directed against the C terminus are employed, and with the antibody 9E10 directed against the c-Myc epitope tag (data not shown).

We used a [^{3}H]GABA uptake assay to determine quantitatively the surface distribution of GAT-3 c-Myc in MDCK cells. Cells were grown on 6.5-mm Costar Transwell filters for 1 week prior to the assay. Labeled GABA was added to either the apical or basolateral media compartments of the Transwell chamber and cells were incubated for 12 min at room temperature (see "Experimental Procedures" for details). Results from the transport assay (Fig. 3) are in good agreement with the immunofluorescence data. GAT-3 c-Myc transport activity is clearly present at both the apical and basolateral surfaces. The ratio of apical to basolateral transport is very close to 1:1 and is independent of the total level of transport. Non-uniform total transport levels most likely reflect variations in transporter expression among cell lines. It is possible that overexpression of GAT-3 c-Myc saturated an apical sorting pathway and that the excess GAT-3 c-Myc was then misdirected to the basolateral surface as a result. It should be noted, however, that several of our wild type GAT-3 cell lines express the GABA transporter at levels greater than our GAT-3 c-Myc cell lines, as determined by comparative Western blotting (data not shown). Despite these high levels of expression, however, all of these cell lines exhibit strict apical polarity, suggesting that we have not attained levels of overexpression sufficient to saturate an apical sorting pathway.

It would appear, therefore, that the addition of the c-Myc epitope tag interferes with the proper sorting and localization of GAT-3. One possible explanation for this surprising behavior is based upon the hypothesis that the tag prevents components of the cellular sorting machinery from recognizing and interacting with an apical sorting signal in the C terminus of GAT-3. According to this model the transporter is mis-sorted to both surfaces as a consequence of this putative steric hindrance. To determine whether such apical sorting information resides within the C terminus of GAT-3, and to rule out the possibility that the c-Myc tag itself acts as a basolateral signal, we prepared a GAT-3 C-terminal truncation construct. In GAT-3 Δ32, the C-terminal 32 amino acids are removed while the rest of the transporter remains entirely intact (Fig. 1). These 32 amino acids comprise approximately half of what is predicted to constitute the C-terminal cytoplasmic tail of GAT-3. GAT-3 Δ32 transporters transiently expressed in COS-1 reach the cell surface and transport GABA, suggesting that this construct is functional and not grossly misfolded (data not shown). Examination of GAT-3 Δ32 stably expressed in MDCK cell lines (more than five independent clones were examined) by immunofluorescence confocal microscopy demonstrated that, like GAT-3 c-Myc, it is present at both the apical and basolateral surfaces (Fig. 2, *g* and *h*). The polarity of several lines of GAT-3 Δ32 examined by GABA transport assay confirmed that the truncated construct is present at both cell surfaces (Fig. 3). The apical to basolateral transport ratio is approximately 1:1 in the GAT-3 Δ32 lines tested. The GAT-3 Δ32 results, combined with the results from the GAT-3 c-Myc construct, render unlikely the possibility that the c-Myc tag itself encodes basolateral sorting information. Instead, these data suggest that there is information required for apical sorting within the C-terminal 32 amino acids of GAT-3. Furthermore, interpretation of this information is apparently impeded or disrupted if additional sequence is appended to the C terminus.

While the C terminus appears to be important for GAT-3 sorting, recent studies have shown that the N terminus of related neurotransmitter transporters are important for their polarized distribution in epithelial cells (28). To determine whether the N terminus might also play a role in GAT-3 sorting we made a transporter construct in which 40 amino acids of the extreme N terminus were deleted. Immunofluorescent confocal microscopy shows that the majority of GAT-3 Δ40N is confined to the apical surface (more than five independent clones), in a pattern similar to that of wild type GAT-3 (Fig. 4, *a* and *b*). GABA transport studies confirm this localization (Fig. 4, *c*). The apical to basolateral transport ratios for several lines of GAT-3 Δ40N are greater than 10:1, similar to what we find in most GAT-3 expressing cell lines (Fig. 3). The average of all the GAT-3 Δ40N cell lines tested is 10.3:1. These results suggest that the N-terminal 40 amino acids of GAT-3 are unlikely to play a major role in determining the distribution of the GAT-3 transporter in MDCK cells.

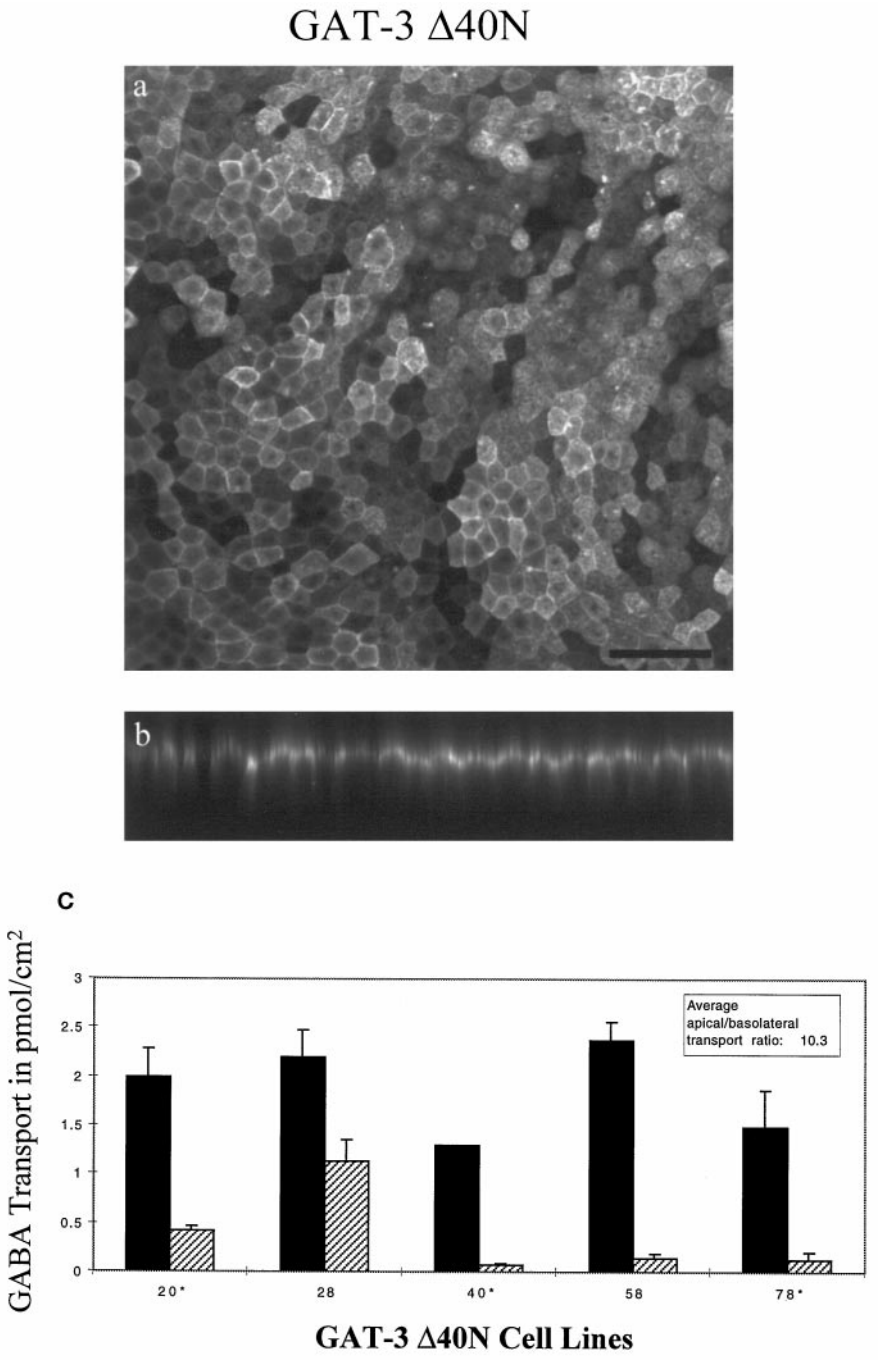

FIG. 4. **Cell surface distribution of the GAT-3 N-terminal deletion construct GAT-3 Δ40N.** MDCK cells stably expressing GAT-3 Δ40N were grown on 24-mm Costar Transwell filters for 1 week and then prepared for immunofluorescence staining using the GAT-3 specific antibody 670 and a FITC-conjugated anti-rabbit secondary antibody. *a* and *b* show confocal en face and *xz* images, respectively, of GAT-3 Δ40N expressing MDCK cells. GAT-3 Δ40N is restricted to the apical surface, similar to wild type GAT-3. *Bar* equals 50 μm. *c* shows GABA transport by cells expressing GAT-3 Δ40N. MDCK cells stably expressing GAT-3 Δ40N were analyzed using the GABA transport assay described in the legend to Fig. 3. The results show that the majority of GABA transport activity is present at the apical surface in these GAT-3 Δ40N cell lines. In most cases the transport activity exhibited by GAT-3 Δ40N cell lines is very similar to what is seen in wild type GAT-3 cell lines. ■, apical; ▨, basolateral. *Asterisk* indicates the average of two independent experiments.

Importance of the C-terminal Cytoplasmic Tail of GAT-2 for its Basolateral Localization—We next wondered whether the basolateral accumulation of GAT-2 is similarly dependent upon information contained within its C-terminal tail. To test this possibility, we generated a GAT-2 C-terminal deletion construct, GAT-2 Δ24, which is identical to wild type GAT-2 except that it lacks its last 24 amino acids (Fig. 1). When GAT-2 Δ24 is expressed stably in MDCK cells, confocal immunofluorescence microscopy, employing the R22 antibody, demonstrated that it is present at both the apical and basolateral surfaces (more than 10 independent clones) (Fig. 5, *a* and *b*). This is distinctly different from the wild type GAT-2 localization pattern (Fig. 5, *c* and *d*) (1). Examination of several GAT-2 Δ24 clones by GABA transport assay shows that the transporter activity is polarized to the apical surface with an average apical to basolateral transport ratio of 4.2:1. Some cell lines exhibit considerably less polarized distributions, with transport ratios in the range of 2:1 (Fig. 5*e*). Apical to basolateral distribution ratios for wild type GAT-2 have previously been shown to be approximately 1:7 (1). These results strongly suggest that the C terminus of GAT-2 contains basolateral sorting information. The fact that the truncated transporter is not equally distributed to both apical and basolateral surfaces may also indicate the presence of apical sorting information which is suppressed or inactive in the intact protein (29).

Di-leucine residues have been identified as sorting and internalization signals for several integral membrane proteins (4, 7, 10, 30–32). The C terminus of GAT-2 contains a di-leucine motif (positions 592 and 593) which is absent in the GAT-2 Δ24 construct. We speculated that the lack of this di-leucine motif could explain the missorting observed with the GAT-2 Δ24 construct. To test this possibility we mutated the leucines at positions 592 and 593 to alanines, and then expressed the mutated GAT-2 transporter, referred to as GAT-2LL>AA, in

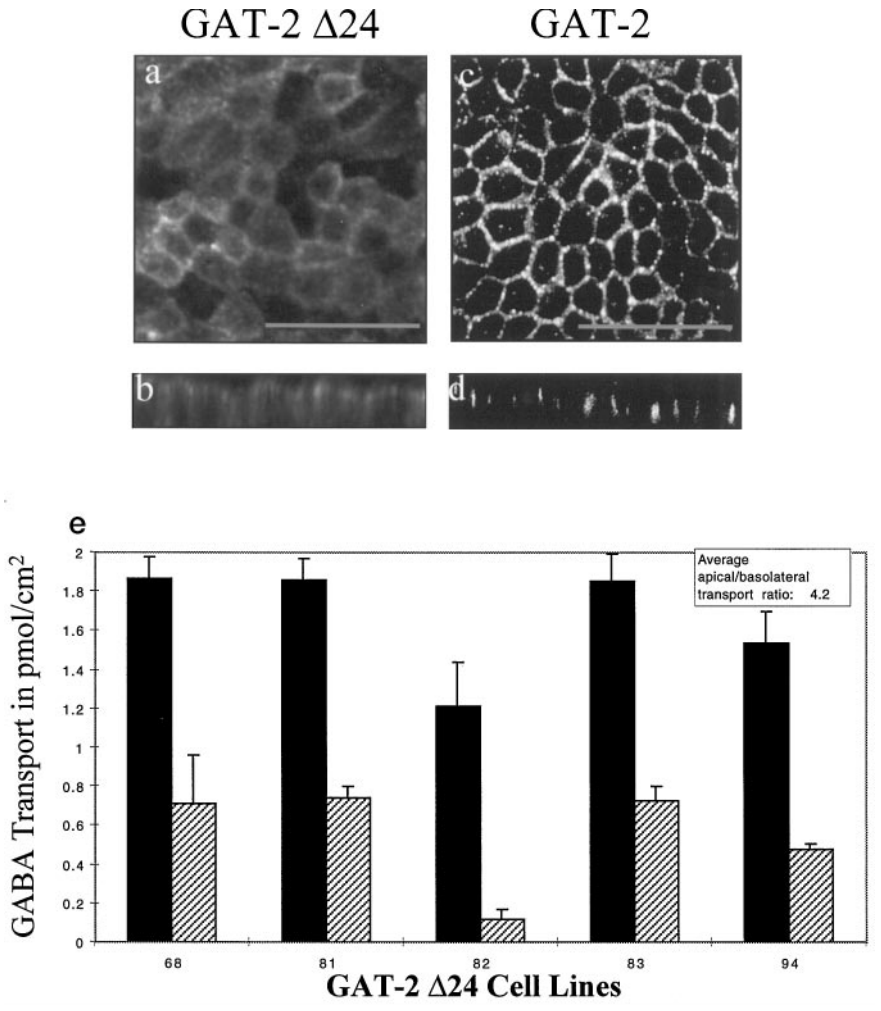

FIG. 5. **Cell surface distribution of the GAT-2 Δ24 chimera.** MDCK cells stably expressing GAT-2 Δ24 were examined by immunofluorescence using the GAT antibody R22 and a FITC-conjugated anti-rabbit secondary antibody. *a* and *b* show confocal en face and *xz* images, respectively, of GAT-2 Δ24 expressing MDCK cells. GAT-2 Δ24 is present at both the apical and basolateral surfaces in contrast to wild type GAT-2 (*c* and *d*) which is basolateral when expressed stably in MDCK cells. *Bar* equals 50 μm in *a* and *c*. *e* shows GABA transport by cells expressing GAT-2 Δ24. The *graph* shows that the majority of the GABA transport activity is present at the apical surface in the GAT-2 Δ24 cell lines, although there is also significant transport activity occurring at the basolateral surface. ■, apical; ▨, basolateral. *Asterisk* indicates the average of two independent experiments.

MDCK cells. Immunofluorescence experiments (Fig. 6, *a* and *b*) demonstrate that GAT-2LL>AA is present predominantly at the basolateral surface. GABA transport studies (Fig. 6*c*) demonstrate that the majority of the transport activity for this mutated transporter is also expressed at the basolateral surface with an apical to basolateral ratio of 1:11. These two lines of evidence suggest that the di-leucine motif present in the C-terminal cytoplasmic tail of GAT-2 does not contribute significantly to achieving the concentration of the transporter at the basolateral surface of polarized epithelia.

The C-terminal Tail of GAT-2 Directs a GAT-3 Chimera to the Basolateral Surface—GAT-2 and GAT-3 are 65% identical and hydropathy plots predict that they both share the same membrane topology (17). These similarities make it possible to generate chimeras between the two transporters without introducing major structural changes (27). We chose to exchange the C-terminal tails between GAT-2 and GAT-3 to determine whether the sorting signals present in these tails could redirect either GABA transporter to the surface of the plasma membrane associated with the transporter which contributes the C-terminal domain.

The first chimera we prepared, GAT-3/C2, replaces the C-terminal amino acids of GAT-3 with the last 22 amino acids of GAT-2 (Fig. 1). When expressed transiently in COS-1 cells, GAT-3/C2 is present at the plasma membrane and capable of transporting GABA (data not shown). Lines of MDCK cells stably expressing GAT-3/C2 were generated and examined by confocal immunofluorescence microscopy. In contrast to the apical distribution of wild type GAT-3, GAT-3/C2 was almost entirely basolateral (more than five independent clones) (Fig. 7, *a* and *b*). This localization pattern is dramatically different from that seen with c-Myc-tagged GAT-3 or GAT-3 Δ32 (Fig. 2). While GAT-3 c-Myc and GAT-3 Δ32 are present equally at both the apical and basolateral surfaces, GAT-3/C2 is restricted exclusively to the basolateral domain. GABA transport studies performed on several lines of GAT-3/C2 show that the vast majority of transport activity is present at the basolateral surface (Fig. 7, *c*). In most cell lines examined, the ratio of apical to basolateral transport was 1:20, which is similar to the transport ratios detected in wild type GAT-2 expressing cell lines (26).

The C-terminal Tail of GAT-3 Has a Weak Effect on the Sorting of a GAT-2 Chimera—We also constructed the reciprocal chimera, GAT-2/C3, which consists of GAT-2 with the C-terminal 32 amino acids of GAT-3 in place of its own C-terminal 22 amino acids (Fig. 1). MDCK cell lines stably expressing the GAT-2/C3 chimera were examined by confocal immunofluorescence microscopy, which reveals that the chimera is present at both the apical and basolateral surfaces (more than five independent cell lines examined) (Fig. 8, *a* and *b*). Quantitation by GABA transport assay performed on several GAT-2/C3 lines indicate that this chimeric transporter exhibits modest to strong polarity, depending on the cell line assayed (Fig. 8*c*). The apical to basolateral transport ratios of these cell lines, in some cases, are indistinguishable from GAT-2 Δ24, whereas other cell lines are nearly as apically polarized as GAT-3. The transport data show that, on average, GAT-2/C3 is more apically localized than GAT-2 Δ24 (apical to basolateral ratio of 6.9:1 *versus* a ratio of 4.2:1, respectively). Clearly, the difference in distribution between the GAT-2 deletion and chimeric con-

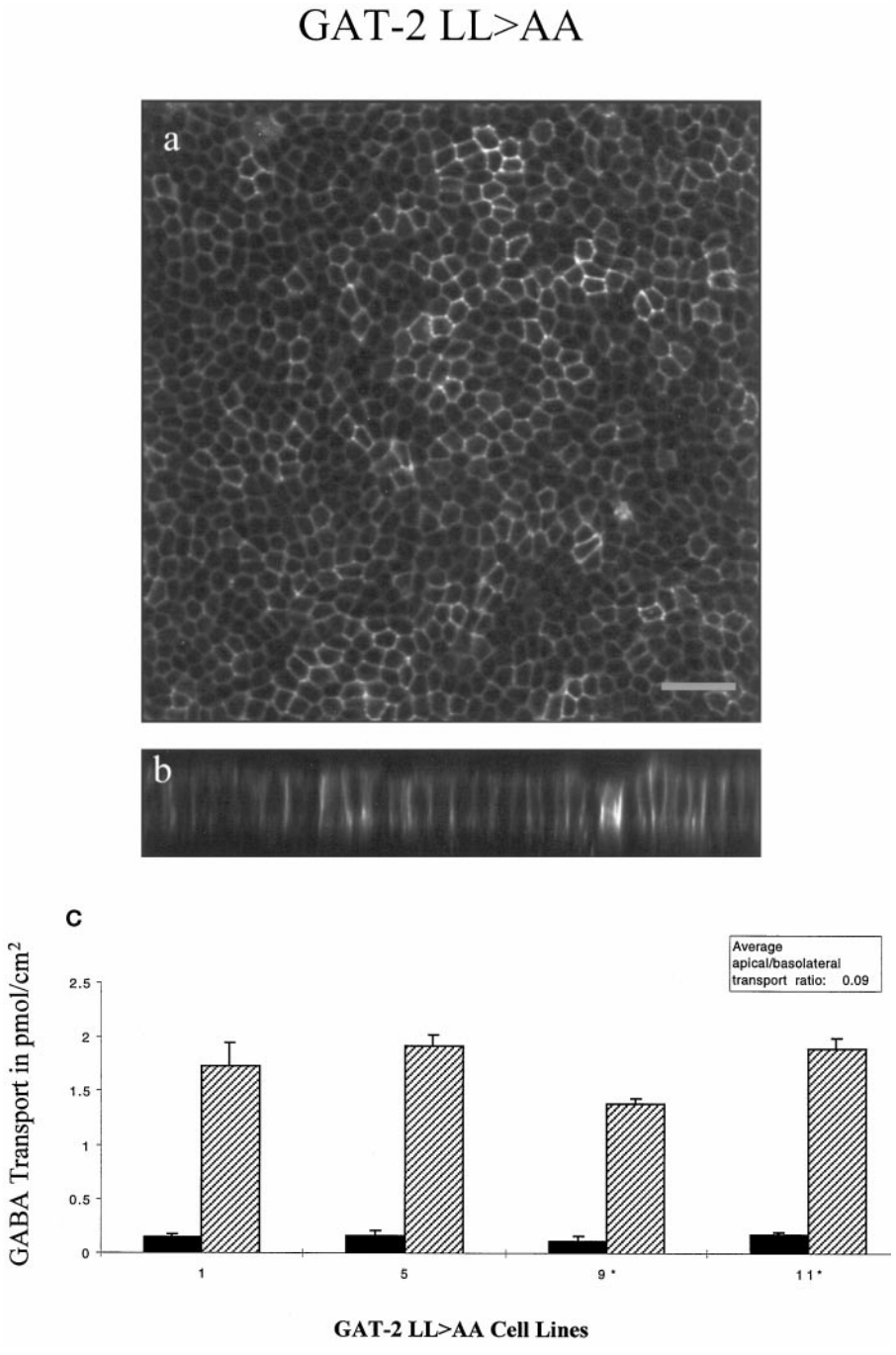

FIG. 6. **Cell surface distribution of the GAT-2 LL>AA transporter.** MDCK cells stably expressing GAT-2 LL>AA were examined by immunofluorescence using the GAT antibody R22 and a FITC-conjugated anti-rabbit secondary antibody. *a* and *b* show confocal en face and *xz* images, respectively, of GAT-2 LL>AA expressing MDCK cells. GAT-2 LL>AA is present at basolateral surface, similar to wild type GAT-2. *Bar* equals 50 μm. *c* shows GABA transport by cells expressing GAT-2 LL>AA. The *graph* shows that the majority of the GABA transport activity is present at the basolateral surface in the GAT-2 LL>AA cell lines, without any significant transport activity occurring at the apical surface. ■, apical; ▨, basolateral. *Asterisk* indicates the average of two independent experiments.

structs, GAT-2 Δ24 and GAT-2/C3, is not as striking as the difference between the GAT-3 deletion and chimeric constructs, GAT-3 Δ32 and GAT-3/C2. These results are, however, consistent with the idea that the GAT-3 C-terminal 32 amino acids may encode apical sorting information. They further suggest that this sequence may interact with or depend upon other domains of the transporter proteins in order to be properly interpreted.

The Three C-terminal Amino Acids of GAT-3 Encode Sorting Information Important for GAT-3s Apical Localization—The C terminus of GAT-3 appears to be important for the apical localization of this transporter in MDCK cells (Figs. 2 and 3). The final residues of this C-terminal tail are threonine, histidine, and phenylalanine (THF), which are reminiscent of the sequences present at the extreme C-terminal tails of proteins known to associate with members of the MAGUK family (33). The MAGUK proteins incorporate one or more copies of the PDZ domain, which is named for three of the proteins in which the sequence homology defining this protein-protein interaction motif were first identified: PSD-95/SAP90, Dlg, and ZO-1 (33). Interactions between the PDZ domain of a MAGUK protein and the extreme cytoplasmic tail of an integral membrane polypeptide appear to be important in organizing the surface distributions of intrinsic membrane proteins. Evidence for this type of protein-protein interaction, and for its ability to regulate the surface distribution of integral membrane proteins, has been identified with the MAGUK family member PSD-95/SAP90 and an NMDA receptor isoform, and in a separate report, with PSD-95/SAP90 and a Shaker-type K^+ channel (34, 35). To investigate whether the extreme C terminus of GAT-3 is important for this protein's sorting, we designed a C-terminal deletion construct in which the last three amino acids were removed (Fig. 1). GAT-3 THF^- transporters expressed stably in MDCK are present at both the apical and basolateral surfaces

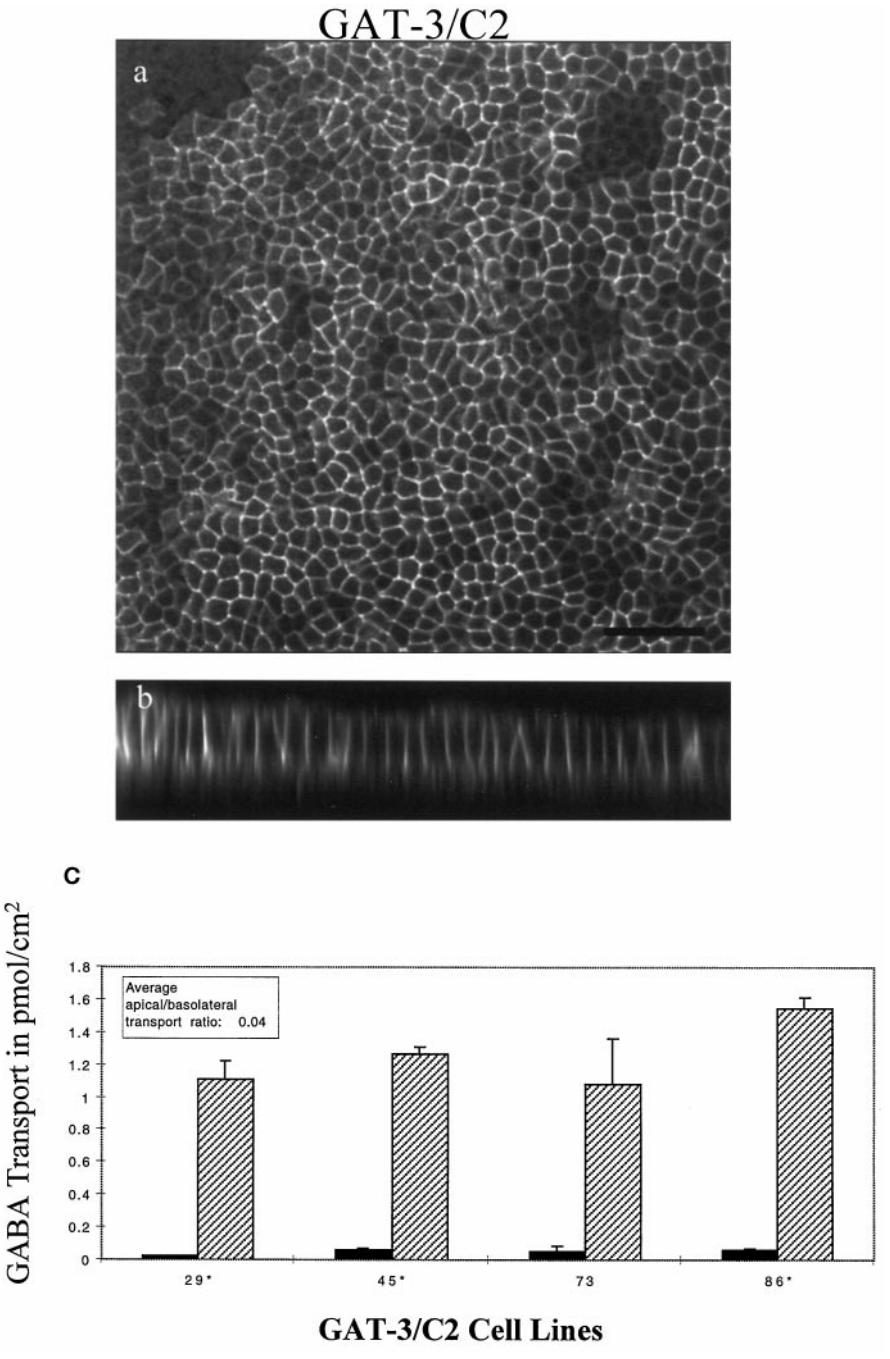

FIG. 7. **Cell surface distribution of the GAT-3/C2 chimera.** MDCK cells stably expressing GAT-3/C2 were grown on 24-mm Costar Transwell filters for 1 week and examined by immunofluorescence using the GAT-3 specific antibody 669 and a FITC-conjugated anti-rabbit secondary antibody. *a* and *b* show confocal en face and *xz* images, respectively, of GAT-3/C2 expressing MDCK cells. GAT-3/C2 is present predominantly at the basolateral surface in sharp contrast to the apical localization of wild type GAT-3. *Bar* equals 50 μm. *c* shows GABA transport by cells expressing GAT-3/C2. The *graph* shows that almost all of the GABA transport activity is present at the basolateral surface in the GAT-3/C2 cell lines. These results are in good agreement with the immunofluorescence data obtained from these GAT-3/C2 cell lines. The *asterisk* (*) indicates cell lines for which the data from two independent experiments have been averaged. ■, apical; ▨, basolateral.

(Fig. 9, *a* and *b*) when examined by immunofluorescence microscopy (more than five independent clones). GABA transport assays confirm that the GAT-3 THF^- transporter is present and functional at both apical and basolateral plasma membrane domains with polarity ratios similar to those observed with the GAT-3 Δ32 and GAT-3 c-Myc constructs (3.2:1, 1.4:1, and 0.9:1, respectively) (Figs. 9*c* and 3). This result suggests that the extreme C terminus is important for GAT-3 sorting, since the effect of the THF^- deletion is nearly as dramatic as removing 32 amino acids from the C terminus (compare the 1.4:1 apical to basolateral ratio of GAT-3 Δ32 and the 3.2:1 ratio for GAT-3 THF^-) (Fig. 9*c*). These observations are consistent with the possibility that the C-terminal THF sequence participates in a protein-protein interaction with a MAGUK protein, or a protein with an analagous role, and that this association plays an important part in ensuring the steady state distribution of GAT-3.

DISCUSSION

We have demonstrated that the GABA neurotransmitter transporters, GAT-2 and GAT-3, both encode information in their C-terminal cytoplasmic tails which is important for their correct sorting within MDCK cells. GAT-2 stably expressed in MDCK cells is restricted to the basolateral surface when examined using indirect immunofluorescence, GABA transport assay, and cell surface biotinylation. In contrast, the highly homologous GAT-3 transporter is found apically in these cells when examined by the same methods (26) (for summary, see Fig. 10). When the 22 C-terminal amino acids of GAT-2 replace the C-terminal 32 amino acids of GAT-3, the resulting GAT-3/C2 chimera is present almost entirely at the basolateral surface (Figs. 7, *a-c*). The GAT-2 Δ24 construct, which lacks the last 24 amino acids of its C terminus, is not sorted to the basolateral surface like GAT-2, but instead is detected at both

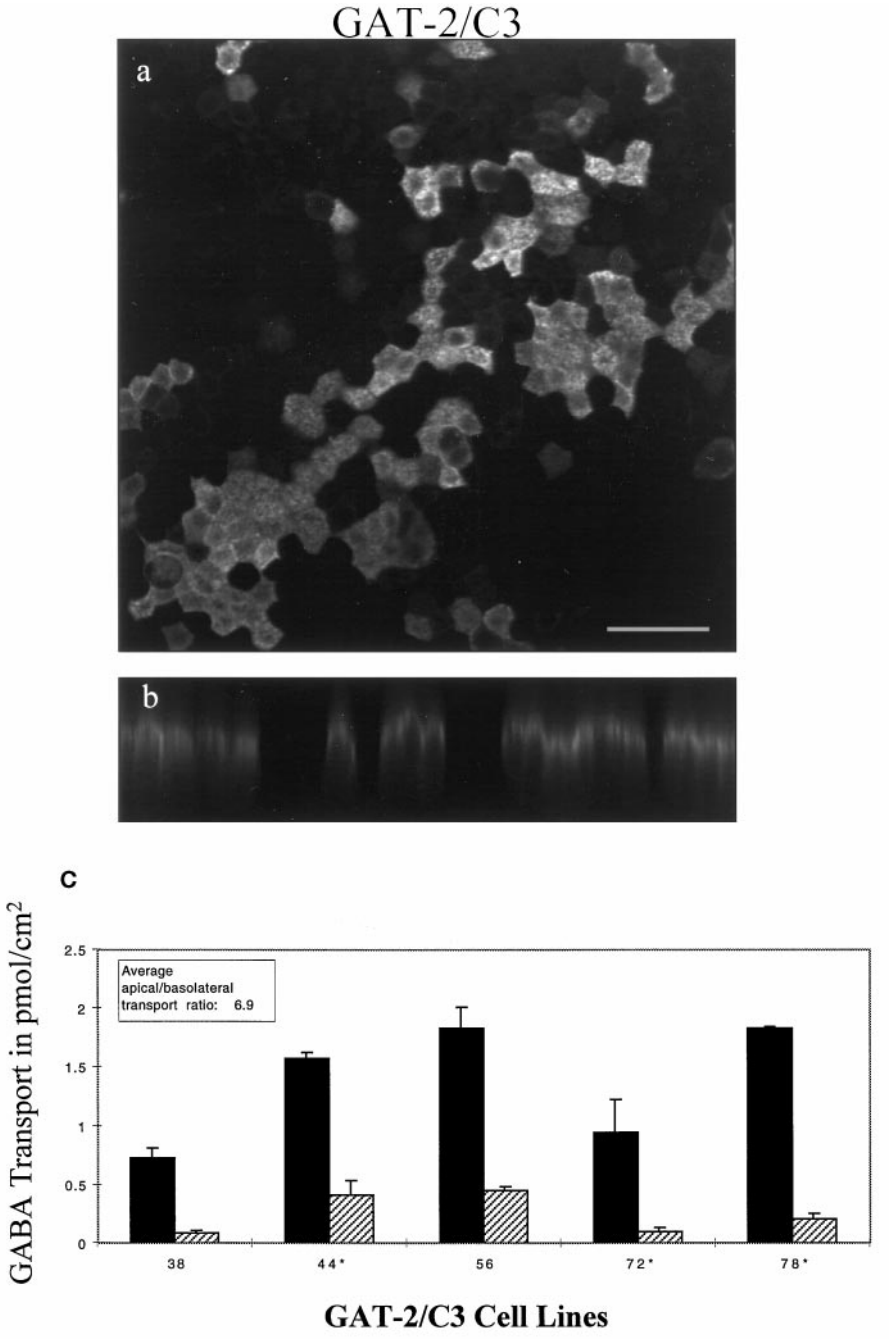

FIG. 8. **Cell surface distribution of the GAT-2/C3 chimera.** MDCK cells stably expressing GAT-2/C3 were grown on 24-mm Costar Transwell filters for 1 week and then prepared for immunofluorescence staining using the GAT-3 specific antibody 670 and a FITC-conjugated anti-rabbit secondary antibody. *a* and *b* show confocal en face and *xz* images, respectively, of GAT-2/C3 expressing MDCK cells. GAT-2/C3 is present predominantly at the apical surface, similar to the localization of wild type GAT-3. GAT-2/C3 is also detected faintly at the lateral surface of these cell lines. *Bar* equals 50 μm. *c* shows GABA transport by cells expressing GAT-2/C3. The *graph* shows that the majority of the GABA transport activity is present at the apical surface in the GAT-2/C3 cell lines, although there is also significant transport activity occurring at the basolateral surface. The apical to basolateral transport ratios exhibited by these cell lines are consistent with a primarily apical localization of the GAT-2/C3 chimera, although the ratios are not as great as those for wild type GAT-3. The *asterisk* (*) indicates cell lines for which the data from two independent experiments have been averaged. ■, apical; ▨, basolateral.

the apical and basolateral surfaces (Figs. 5, *a, b,* and *e*). These two results strongly suggest the existence of a potent basolateral sorting signal in the last 22 amino acids of the GAT-2 transporter. Examination of this sequence reveals the presence of a di-leucine motif at positions 592 and 593 which is transferred to GAT-3 in the GAT-3/C2 construct and which is absent from the GAT-2 Δ24 construct (Fig. 1). Since di-leucine motifs are capable of mediating basolateral sorting when presented in the context of single-pass membrane proteins (7, 10, 31), we tested whether these residues are responsible for the basolateral targeting of GAT-2. Replacement of both leucine residues with alanines had no effect on the basolateral accumulation of GAT-2. These data indicate that a novel basolateral sorting signal may reside within the 24 amino acids of the GAT-2 tail.

The importance of the C-terminal cytoplasmic tail of GAT-3 in determining its apical sorting was revealed after a 10-amino acid epitope tag was added to the C terminus of this transporter. The addition of the c-Myc epitope tag caused missorting of GAT-3 transporters to both the apical and basolateral surfaces (Figs. 2, *e* and *f*, and 3). This unexpected result suggests that future functional or targeting studies employing epitope-tagged proteins must be interpreted with some degree of caution, since addition of small, and seemingly unremarkable, sequences can dramatically alter the behavior of the tagged protein. It must also be noted, however, that the missorting attributable to the placement of the c-Myc tag provided fortuitous insight into the nature of GAT-3s apical sorting information.

Removing 32 amino acids from the C terminus of GAT-3 had the same affect as the c-Myc tag on the protein's localization (Figs. 2, *g* and *h*, and 3). When these 32 residues from the GAT-3 C terminus were substituted for the GAT-2 C-terminal cytoplasmic tail, creating the GAT-2/C3 chimera, a significant fraction of the chimeric constructs were sorted to the apical surface (Figs. 8, *a-c*). It is difficult to assess whether the GAT-3 C terminus drives the apical sorting of GAT-2/C3, since GAT-2

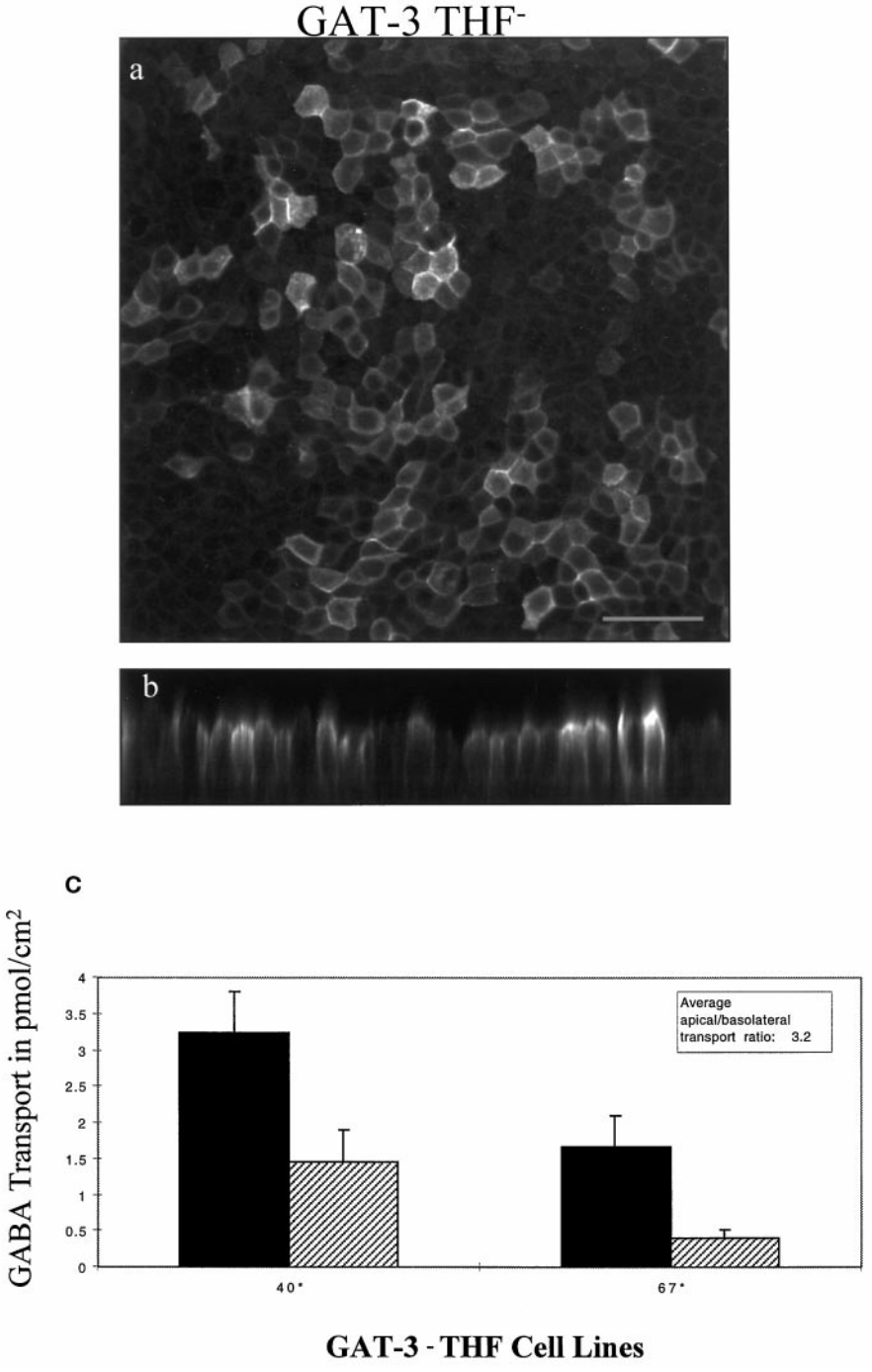

FIG. 9. **Cell surface distribution of the GAT-3 THF⁻ chimera.** MDCK cells stably expressing GAT-3 THF⁻ were examined by immunofluorescence using the GAT-3 specific antibody 670 and a FITC-conjugated anti-rabbit secondary antibody. *a* and *b* show confocal en face and *xz* images, respectively, of GAT-3 THF⁻ expressing MDCK cells. GAT-3 THF⁻ is present at both the apical (■) and basolateral (▨) surface in contrast to the apical localization of wild type GAT-3. *Bar* equals 50 μm. *c* shows GABA transport by cells expressing GAT-3 THF⁻. The graph shows that the GABA transport activity is present at both the apical and basolateral surfaces in the GAT-3 THF⁻ cell lines. The apical to basolateral transport ratios of GAT-3 THF⁻ cell lines are much smaller than those found in GAT-3 wild type cell lines. The *asterisk* (*) indicates cell lines for which the data from two independent experiments have been averaged.

Δ24 is also predominantly apical. It should be noted, however, that quantitative transport measurements indicate that the apical to basolateral ratio is higher for GAT-2/C3 than for GAT-2 Δ24 (6.9:1 and 4.2:1 respectively) (Figs. 5*e* and 8*c*). Perhaps the simplest explanation for these results is that GAT-2 embodies weak apical sorting information within some aspect of its structure. Consequently, when it is deprived of its basolateral sorting signal, it is distributed to both surfaces but with an apical predominance.

While it appears that appending the GAT-3 C-terminal tail to GAT-2 Δ24 exerts a measurable affect on apical sorting, it is also clear that the sorting information contributed by the GAT-3 tail alone is not sufficient to mediate full apical targeting. It is possible, therefore, that the apical signal of GAT-3 extends beyond the 32 amino acids we have examined, or that it is bipartite, with another critical domain residing elsewhere in the protein. Consistent with this possibility, the presence of sorting information residing outside the C terminus has been demonstrated for GAT-1 (36) and for biogenic amine transporters.[2] Finally, it has been suggested that apical targeting may in part be mediated by lectins which interact with the sugar moieties found on the substrate protein's lumenal extensions (36–39). This does not seem likely to be the case for GAT-3, since the potential sites for *N*-linked glycosylation on its second extracellular loop are well conserved in the basolateral GAT-2 transporter (17).

Our data suggest that the default pathway carries membrane proteins lacking sorting determinants to both surface domains in MDCK cells. Previous studies, by Odorizzi *et al.*

[2] H. Gu and G. Rudnick, personal communication.

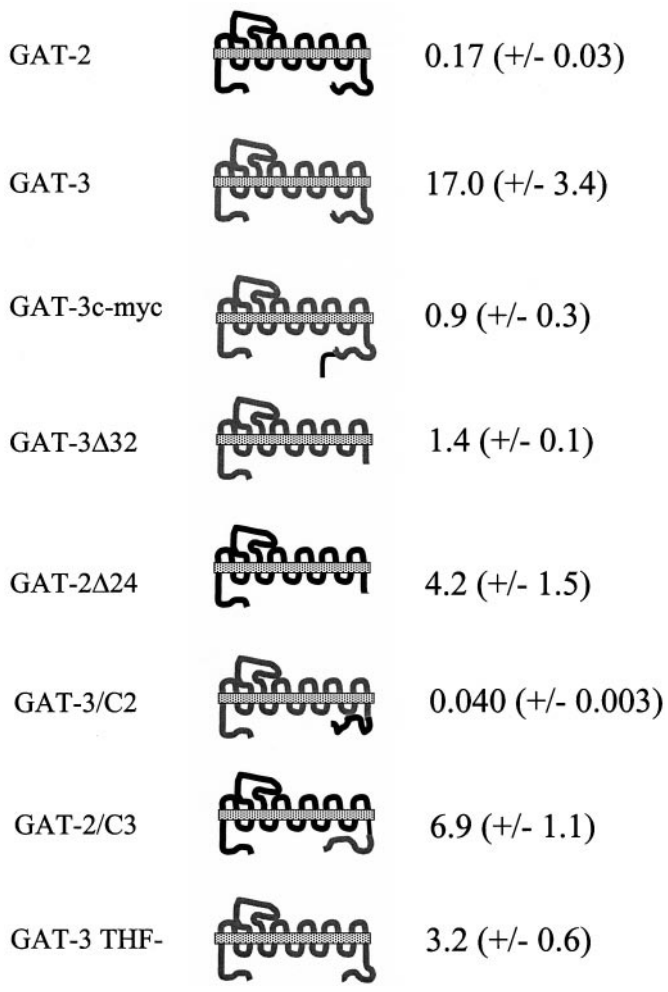

FIG. 10. **Summary of the cell surface distributions of the GAT deletion and chimeric constructs.** Schematic diagrams of each GAT transporter construct are presented. GAT-2 is drawn in *black* while GAT-3 is in *gray* (the *thin black line* represents the 10 amino acid c-Myc epitope tag). The *stippled bar* represents the plasma membrane. In the *right column* the apical to basolateral GABA transport ratios for each construct are tabulated. The values for standard errors of the mean are shown in *parentheses*.

(29), of the transferrin receptor, which normally has a predominantly basolateral steady state distribution in MDCK cells, demonstrate that when this protein is deprived of the basolateral sorting signal encoded in its cytoplasmic tail it is distributed to both the apical and basolateral membranes (29). Our findings with GAT-3 Δ32 and GAT-3 c-Myc are consistent with this behavior. These authors further proposed that the tendency of certain proteins, such as the low density lipoprotein receptor, to accumulate at the apical surface when deprived of their normal basolateral signals is attributable to the presence of cryptic apical sorting information in the remaining protein sequence. Similarly, as noted above, we believe that the moderate polarization of GAT-2 Δ24 to the apical surface does not imply the existence of an apical default pathway, but rather indicates that an apical sorting signal may have been engaged or exposed by truncating the C terminus of GAT-2.

Recently the kv1.4 K^+ channel and a NMDA receptor isoform have been shown to interact with PSD-95/SAP90, a member of the MAGUK family (34, 35, 40). Additionally, AMPA receptors and metabatropic glutamate receptors have been found to interact with the PDZ domains of other MAGUK family members (41, 42). These interactions take place between specific amino acids at the extreme C-terminal tail of the integral membrane proteins and a domain within the MAGUK family member (33, 41–44). In general, the extreme C-terminal sequences of transmembrane proteins which interact with MAGUK family members take the form of (S/T)*X*Z, where *X* can be any amino acid and Z tends to be a hydrophobic residue (34, 35). In this context, the behavior of the GAT-3 THF^- construct is intriguing. Removing the three extreme C-terminal residues (threonine, histidine, and phenylalanine) leads to a mislocalization of the mutant transporter to both the apical and basolateral cell surfaces (Figs. 9, *a-c*). It is tempting to hypothesize that these three residues of GAT-3 participate in interactions with the PDZ domain of a MAGUK protein and that this interaction is required for GAT-3s steady-state apical distribution. Comparison of the C-terminal residues of GAT-3 with peptide sequences which have been shown to bind to PDZ domains suggests that GAT-3 is a good candidate for such an association (44). The missorting of GAT-3 c-Myc is also consistent with the possibility that residues at the extreme C-terminal tail participate in interactions important for the transporters proper sorting. The addition of an epitope tag may prevent the necessary recognition of the THF sequence by a MAGUK protein from occurring. The hypothesis that there may be an interaction between GAT-3 and PSD-95/SAP90 or a related family member is especially attractive since PSD-95/SAP90 was identified as a postsynaptic density protein in GABAergic neurons (40). However, preliminary experiments using PSD-95/SAP90 in a co-clustering assay in COS-1 cells assay did not provide evidence of an interaction between GAT-3, GAT-2, or the betaine transporter, BGT-1, with this MAGUK (data not shown). It may be that members of the GABA transporter family interact with MAGUKs other than PSD-95/SAP90, or that the interactions are too weak to be detected by this assay in COS-1 cells. The dramatic affect on sorting caused by removing only three amino acids from the C terminus of GAT-3 does, however, justify a future search for possible interactions with MAGUK family members. The role served by PDZ domain-containing proteins in clustering ion channels and integral membrane receptors might be readily adapted to a function in generating or maintaining the polarized distributions of membrane proteins in both epithelia and neurons. GABA transporters exhibit a well defined polarity in both of these cell types, which may possibly be the result of stabilizing interactions with MAGUKs or MAGUK-like proteins.

GAT-2 and GAT-3 are not endogenous to MDCK cells; however, a closely related GABA transporter family member, BGT-1, is expressed endogenously in this epithelial cell type (19, 45). Additionally, GAT-2 has been localized to the basolateral domain of retinal pigmented epithelia and GAT-2 mRNA is present in kidney, liver, and leptomeningial epithelial cells (17, 18, 46, 47). Although the GABA transporters are most often thought of as being localized to terminal neuronal processes and glial cells, where they function to clear the synapse of the inhibitory GABA neurotransmitter, it is evident that they also function in epithelia. It is possible that GAT-2 may protect cells from hyperosmotic conditions by importing betaine or another osmolyte, as BGT-1 does in the outer medulla of the kidney (19, 45). It is also interesting to note that both GAT-2 and BGT-1, which are endogenously expressed in epithelial cells, are both basolateral when synthesized in MDCK cells. In contrast, GAT-1 and GAT-3, which are both found in the axonal projections of several populations of neurons, are apical when expressed in MDCK cells (18, 23, 24). These observations are consistent with the model which predicts that the axons of neurons may be analogous to the apical surfaces of epithelia, while the somatodendritic domain of neurons is similar to the basolateral surface of epithelia (2). Exogenous expression of our

chimeric transporters in neurons will allow us to determine whether the same molecular domains are required for sorting in both cell types.

Acknowledgments—We are grateful to Drs. B. Kanner, L. Borden, R. Jahn, L. Edelmann, C. Garner, and S. Goldstein for kindly providing reagents used in this study. We are also indebted to Drs. G. Rudnick and H. Gu for help in performing the GABA transport assays and Daniel Zahler for his contributions to the preparation of the GAT-2 LL>AA construct. Finally, we acknowledge the insight and support provided by all of the members of the Caplan lab while these studies were being performed.

REFERENCES

1. Caplan, M. J. (1997) *Am. J. Physiol.* **272,** F425–F429
2. Simons, K., Dupree, P., Fiedler, K., Huber, L. A., Kobayashi, T., Kurzchalia, T., Olkkonen, V., Pimplikar, S., Parton, R., and Dotti, C. (1992) *Cold Spring Harbor Symp. Quant. Biol.* **57,** 611–619
3. Rodriguez-Boulan, E., and Powell, S. K. (1992) *Annu. Rev. Cell Biol.* **8,** 395–427
4. Matter, K., Yamamoto, E. M., and Mellman, I. (1994) *J. Cell Biol.* **126,** 991–1004
5. Casanova, J. E., Apodaca, G., and Mostov, K. E. (1991) *Cell* **66,** 65–75
6. Okamoto, C. T., Shia, S. P., Bird, C., Mostov, K. E., and Roth, M. G. (1992) *J. Biol. Chem.* **267,** 9925–9932
7. Marks, M. S., Woodruff, L., Ohno, H., and Bonifacino, J. S. (1996) *J. Cell Biol.* **135,** 341–354
8. Matter, K., and Mellman, I. (1994) *Curr. Opin. Cell Biol.* **6,** 545–554
9. Brewer, C. B., and Roth, M. G. (1991) *J. Cell Biol.* **114,** 413–421
10. Hunziker, W., and Fumey, C. (1994) *EMBO J.* **13,** 2963–2967
11. Matter, K., Hunziker, W., and Mellman, I. (1992) *Cell* **71,** 741–753
12. Dotti, C. G., and Simons, K. (1990) *Cell* **62,** 63–72
13. Dotti, C. G., Parton, R. G., and Simons, K. (1991) *Nature* **349,** 158–161
14. Pietrini, G., Matteoli, M., Banker, G., and Caplan, M. J. (1992) *Proc. Natl. Acad. Sci. U. S. A.* **89,** 8414–8418
15. Haass, C., Koo, E. H., Teplow, D. B., and Selkoe, D. J. (1994) *Proc. Natl. Acad. Sci. U. S. A.* **91,** 1564–1568
16. Ferreira, A., Caceres, A., and Kosik, K. S. (1993) *J. Neurosci.* **13,** 3112–3123
17. Borden, L. A., Smith, K. E., Hartig, P. R., Branchek, T. A., and Weinshank, R. L. (1992) *J. Biol. Chem.* **267,** 21098–21104
18. Borden, L. A. (1996) *Neurochem. Int.* **29,** 335–356
19. Yamauchi, A., Uchida, S., Kwon, H. M., Preston, A. S., Robey, R. B., Garcia-Perez, A., Burg, M. B., and Handler, J. S. (1992) *J. Biol. Chem.* **267,** 649–652
20. Guastella, J., Nelson, N., Nelson, H., Czyzyk, L., Keynan, S., Miedel, M. C., Davidson, N., Lester, H. A., and Kanner, B. I. (1990) *Science* **249,** 1303–1306
21. Kanner, B. I. (1983) *Biochim. Biophys. Acta* **726,** 293–316
22. Iversen, L. L. (1971) *Br. J. Pharmacol.* **41,** 571–591
23. Pietrini, G., Suh, Y. J., Edelmann, L., Rudnick, G., and Caplan, M. J. (1994) *J. Biol. Chem.* **269,** 4668–4674
24. Radian, R., Ottersen, O. P., Storm-Mathisen, J., Castel, M., and Kanner, B. I. (1990) *J. Neurosci.* **10,** 1319–1330
25. Radian, R., and Kanner, B. I. (1983) *Biochemistry* **22,** 1236–1241
26. Ahn, J., Mundigl, O., Muth, T. R., Rudnick, G., and Caplan, M. J. (1996) *J. Biol. Chem.* **271,** 6917–6924
27. Gottardi, C. J., and Caplan, M. J. (1993) *J. Cell Biol.* **121,** 283–293
28. Perego, C., Bulbarelli, A., Longhi, R., Caimi, M., Villa, A., Caplan, M. J., and Pietrini, G. (1997) *J. Biol. Chem.* **272,** 6584–6592
29. Odorizzi, G., Pearse, A., Domingo, D., Trowbridge, I. S., and Hopkins, C. R. (1996) *J. Cell Biol.* **135,** 139–152
30. Pond, L., Kuhn, L. A., Teyton, L., Schutze, M. P., Tainer, J. A., Jackson, M. R., and Peterson, P. A. (1995) *J. Biol. Chem.* **270,** 19989–19997
31. Heilker, R., Manning-Krieg, U., Zuber, J. F., and Spiess, M. (1996) *EMBO J.* **15,** 2893–2899
32. Dietrich, J., Hou, X., Wegener, A. M., Pedersen, L. O., Odum, N., and Geisler, C. (1996) *J. Biol. Chem.* **271,** 11441–11448
33. Fanning, A. S., and Anderson, J. M. (1996) *Curr. Biol.* **6,** 1385–1388
34. Kim, E., Niethammer, M., Rothschild, A., Jan, Y. N., and Sheng, M. (1995) *Nature* **378,** 85–88
35. Kornau, H. C., Schenker, L. T., Kennedy, M. B., and Seeburg, P. H. (1995) *Science* **269,** 1737–1740
36. Fiedler, K., and Simons, K. (1995) *Cell* **81,** 309–312
37. Fiedler, K., Parton, R. G., Kellner, R., Etzold, T., and Simons, K. (1994) *EMBO J.* **13,** 1729–1740
38. Fiedler, K., and Simons, K. (1994) *Cell* **77,** 625–626
39. Scheiffele, P., Peranen, J., and Simons, K. (1995) *Nature* **378,** 96–98
40. Kistner, U., Wenzel, B. M., Veh, R. W., Cases-Langhoff, C., Garner, A. M., Appeltauer, U., Voss, B., Gundelfinger, E. D., and Garner, C. C. (1993) *J. Biol. Chem.* **268,** 4580–4583
41. Dong, H., O'Brien, R. J., Fung, E. T., Lanahan, A. A., Worley, P. F., and Huganir, R. L. (1997) *Nature* **386,** 279–284
42. Brakeman, P. R., Lanahan, A. A., O'Brien, R., Roche, K., Barnes, C. A., Huganir, R. L., and Worley, P. F. (1997) *Nature* **386,** 284–288
43. Saras, J., and Heldin, C. H. (1996) *Trends Biochem. Sci.* **21,** 455–458
44. Songyang, Z., Fanning, A. S., Fu, C., Xu, J., Marfatia, S. M., Chishti, A. H., Crompton, A., Chan, A. C., Anderson, J. M., and Cantley, L. C. (1997) *Science* **275,** 73–77
45. Kwon, H. M. (1996) *Biochem. Soc. Trans.* **24,** 853–856
46. Durkin, M. M., Smith, K. E., Borden, L. A., Weinshank, R. L., Branchek, T. A., and Gustafson, E. L. (1995) *Brain Res. Mol. Brain Res.* **33,** 7–21
47. Johnson, J., Chen, T. K., Rickman, D. W., Evans, C., and Brecha, N. C. (1996) *J. Comp. Neurol.* **375,** 212–224

Identification of Sorting Determinants in the C-terminal Cytoplasmic Tails of the γ -Aminobutyric Acid Transporters GAT-2 and GAT-3

Theodore R. Muth, Jinhi Ahn and Michael J. Caplan

J. Biol. Chem. 1998, 273:25616-25627.
doi: 10.1074/jbc.273.40.25616